

# Lower Bounds for Planar Electrical Reduction\*

Hsien-Chih Chang      Jeff Erickson  
University of Illinois at Urbana-Champaign  
[hchang17](mailto:hchang17@illinois.edu), [jeffe](mailto:jeffe@illinois.edu)@illinois.edu

Submitted to SODA 2018 — July 12, 2017

## Abstract

We improve our earlier lower bounds on the number of *electrical transformations* required to reduce an  $n$ -vertex plane graph in the worst case [SOCG 2016] in two different directions. Our previous  $\Omega(n^{3/2})$  lower bound applies only to *facial* electrical transformations on plane graphs with *no terminals*. First we provide a stronger  $\Omega(n^2)$  lower bound when the graph has two or more terminals, which follows from a quadratic lower bound on the number of homotopy moves in the annulus, described in a companion paper. Our second result extends our earlier  $\Omega(n^{3/2})$  lower bound to the wider class of *planar* electrical transformations, which preserve the planarity of the graph but may delete cycles that are not faces of the given embedding. This new lower bound follows from the observation that the *defect* of the medial graph of a planar graph is the same for all its planar embeddings.

---

\*This work was partially supported by NSF grant CCF-1408763.

## 1 Introduction

Consider the following set of local operations performed on any graph:

- *Leaf contraction*: Contract the edge incident to a vertex of degree 1.
- *Loop deletion*: Delete the edge of a loop.
- *Series reduction*: Contract either edge incident to a vertex of degree 2.
- *Parallel reduction*: Delete one of a pair of parallel edges.
- *$Y \rightarrow \Delta$  transformation*: Delete a vertex of degree 3 and connect its neighbors with three new edges.
- *$\Delta \rightarrow Y$  transformation*: Delete the edges of a 3-cycle and join the vertices of the cycle to a new vertex.

These operations and their inverses, which we call *electrical transformations* following Colin de Verdière *et al.* [11], have been used for over a century to analyze electrical networks [25]. Steinitz [31,32] proved that any planar network can be reduced to a single vertex using these operations. Several decades later, Epifanov [15] proved that any planar graph with two special vertices called *terminals* can be similarly reduced to a single edge between the terminals; simpler algorithmic proofs of Epifanov’s theorem were later given by Feo [17], Truemper [33,34], and Feo and Provan [18]. These results have since been extended to planar graphs with more than two terminals [3,12,19,20] and to some families of non-planar graphs [19,35].

Despite decades of prior work, the complexity of the reduction process is still poorly understood. Steinitz’s proof implies that  $O(n^2)$  electrical transformations suffice to reduce any  $n$ -vertex planar graph to a single vertex; Feo and Provan’s algorithm reduces any 2-terminal planar graph to a single edge in  $O(n^2)$  steps. While these are the best upper bounds known, several authors have conjectured that they can be improved. Without any restrictions on which transformations are permitted, the only known lower bound is the trivial  $\Omega(n)$ . However, we recently proved that if all electrical transformations are required to be *facial*, meaning any deleted cycle must be a face of the given embedding, then reducing a plane graph without terminals to a single vertex requires  $\Omega(n^{3/2})$  steps in the worst case [8].

In this paper, we extend our earlier lower bound in two directions. First, in Section 3, we consider plane graphs with two terminals. In this setting, leaf deletions, series reductions, and  $Y \rightarrow \Delta$  transformations that delete terminals are forbidden. We prove in Section 3 that  $\Omega(n^2)$  facial electrical transformations are required in the worst case to reduce a 2-terminal plane graph *as much as possible*. Not every 2-terminal plane graph can be reduced to a single edge between the terminals using only facial electrical transformations. However, we show that any 2-terminal plane graph can be reduced to a unique minimal graph called a *bullseye* using a finite number of facial electrical transformations. Our lower bound ultimately reduces to a recent  $\Omega(n^2)$  lower bound on the number of homotopy moves required to simplify a contractible closed curve in the annulus, which we describe in a companion paper [10].

In Section 4, we consider a wider class of electrical transformations that preserve the planarity of the graph, but are not necessarily facial. Our second main result is that  $\Omega(n^{3/2})$  planar electrical transformations are required to reduce a planar graph (without terminals) to a single vertex in the worst case. Like our earlier lower bound for *facial* electrical transformations, our proof ultimately reduces to a study of a certain curve invariant, called the *defect*, of the medial graph (viewed as a closed curve) of the given plane graph  $G$ . A key step in our new proof is the following surprising observation: Although the definition of the medial graph of  $G$  depends on the embedding of  $G$ , the defect of the medial graph is the same for all planar embeddings of  $G$ .

## 2 Background

### 2.1 Types of Electrical Transformations

We distinguish between three increasingly general types of electrical transformations in plane graphs: *facial*, *planar*, and *arbitrary*. (For ease of presentation, we assume throughout the paper that plane graphs are actually embedded on the *sphere* instead of the plane.)

An electrical transformation in a plane graph  $G$  is *facial* if any deleted cycle is a face of  $G$ . All leaf contractions, series reductions, and  $Y \rightarrow \Delta$  transformations are facial, but loop deletions, parallel reductions, and  $\Delta \rightarrow Y$  transformations may not be facial. Facial electrical transformations form three dual pairs, as shown in Figure 2.1; for example, any series reduction in  $G$  is equivalent to a parallel reduction in the dual graph  $G^*$ .

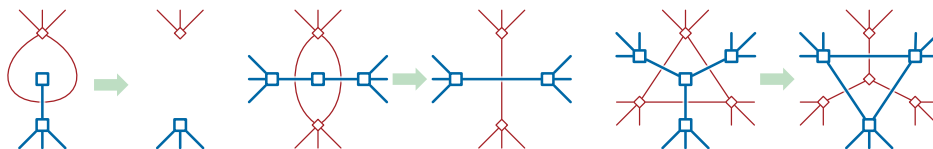


**Figure 2.1.** Facial electrical transformations in a plane graph  $G$  and its dual  $G^*$ .

An electrical transformation in  $G$  is *planar* if it preserves the planarity of the underlying graph. Equivalently, an electrical transformation is planar if the vertices of the cycle deleted by the transformation are all incident to a common face (in the given embedding) of  $G$ . All facial electrical transformations are trivially planar, as are all loop deletions and parallel reductions. The only non-planar electrical transformation is a  $\Delta \rightarrow Y$  transformation whose three vertices are *not* incident to a common face; any such transformation introduces a  $K_{3,3}$  minor into the graph, connecting the three vertices of the  $\Delta$  to an interior vertex, an exterior vertex, and the new  $Y$  vertex.

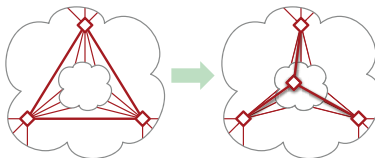


**Figure 2.2.** A non-planar  $\Delta \rightarrow Y$  transformation.

### 2.2 Multicurves and Medial Graphs

Formally, a *closed curve* in a surface  $M$  is a continuous map  $\gamma: S^1 \rightarrow M$ . A closed curve is *simple* if it is injective. A *multicurve* is a collection of one or more disjoint closed curves. We consider only *generic* closed curves and multicurves, which are injective except at a finite number of (self-)intersections, each of which is a transverse double point. A multicurve is *connected* if its image in the surface is connected; we consider only connected multicurves in this paper. The image of any (non-simple, connected) multicurve has a natural structure as a 4-regular map, whose *vertices* are the self-intersection points of the curve, *edges* are maximal subpaths between vertices, and *faces* are components of the complement of the curve in the surface. We do not distinguish between multicurves whose images are combinatorially equivalent maps.

The *medial graph*  $G^\times$  of a plane graph  $G$  is another plane graph whose vertices correspond to the edges of  $G$ , and two vertices of  $G^\times$  are connected by an edge if the corresponding edges in  $G$  are consecutive in cyclic order around some vertex, or equivalently, around some face in  $G$ . Every vertex in every medial graph has degree 4; thus, every medial graph is the image of a multicurve. Conversely, the

1 image of every non-simple multicurve on the sphere is the medial graph of some plane graph. We call a  
 2 plane graph  $G$  *unicursal* if its medial graph  $G^\times$  is the image of a single closed curve.

3 **Smoothing** a multicurve  $\gamma$  at a vertex  $x$  replaces the intersection of  $\gamma$  with a small neighborhood  
 4 of  $x$  with two disjoint simple paths, so that the result is another 4-regular plane graph. There are two  
 5 possible smoothings at each vertex. More generally, a **smoothing** of  $\gamma$  is any multicurve obtained by  
 6 smoothing a subset of its vertices. For any plane graph  $G$ , the smoothings of the medial graph  $G^\times$  are  
 7 precisely the medial graphs of minors of  $G$ .

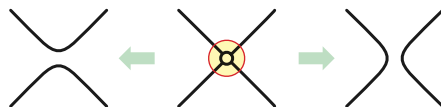


Figure 2.3. Smoothing a vertex.

8 **2.3 Local Moves**

9 A **homotopy** between two curves  $\gamma$  and  $\gamma'$  on the same surface is a continuous deformation from one  
 10 curve to the other, formally defined as a continuous function  $H: S^1 \times [0, 1] \rightarrow M$  such that  $H(\cdot, 0) = \gamma$   
 11 and  $H(\cdot, 1) = \gamma'$ . The definition of homotopy extends naturally to multicurves. Classical topological  
 12 arguments imply that two multicurves are homotopic if and only if one can be transformed into the  
 13 other by a finite sequence of **homotopy moves**, shown in Figure 2.4. A multicurve is **homotopically**  
 14 **reduced** if no sequence of homotopy moves leads to a multicurve with fewer vertices.



Figure 2.4. Homotopy moves 1→0, 2→0, and 3→3.

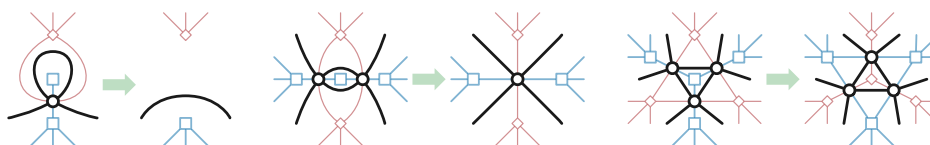


Figure 2.5. Medial electrical moves 1→0, 2→1, and 3→3.

15 Facial electrical transformations in any plane graph  $G$  induce local transformations in the medial  
 16 graph  $G^\times$  that closely resemble homotopy moves. We call these **1→0**, **2→1**, and **3→3** moves, where the  
 17 numbers before and after each arrow indicate the number of local vertices before and after the move;  
 18 see Figure 2.5. We collectively refer to these transformations and their inverses as **medial electrical**  
 19 **moves**. A multicurve is **electrically reduced** if no sequence of medial electrical moves leads to another  
 20 multicurve with fewer vertices.

21 For multicurves on surfaces with boundary, both homotopy moves and medial electrical moves on  
 22 boundary faces are forbidden.

23 **3 Two-Terminal Plane Graphs**

24 Most applications of electrical reductions, starting with Kennelly’s classical computation of effective  
 25 resistance [25], designate two vertices of the input graph as *terminals* and require a reduction to a  
 26 single edge between those terminals. In this context, electrical transformations that delete either of the  
 27 terminals are forbidden; specifically: leaf contractions when the leaf is a terminal, series reductions when  
 28 the degree-2 vertex is a terminal, and  $Y \rightarrow \Delta$  transformations when the degree-3 vertex is a terminal.

1 Epifanov [15] was the first to prove that any 2-terminal planar graph can be reduced to a single  
 2 edge between the terminals using a finite number of electrical transformations, roughly 50 years after  
 3 Steinitz proved the corresponding result for planar graphs without terminals [31, 32]. Epifanov’s proof  
 4 is non-constructive; algorithms for reducing 2-terminal planar graphs were later described by Feo [17],  
 5 Truemper [33], and Feo and Provan [18]. (An algorithm in the spirit of Steinitz’s reduction proof can  
 6 also be derived from results of de Graaf and Schrijver [21].)

7 An important subtlety that complicates both Epifanov’s proof and its algorithmic descendants is  
 8 that not every 2-terminal planar graph can be reduced to a single edge using only *facial* electrical  
 9 transformations. The simplest bad example is the three-vertex graph shown in Figure 3.1; the solid  
 10 vertices are the terminals. Although this graph has more than one edge, it has no reducible leaves, empty  
 11 loops, cycles of length 2 or 3, or vertices with degree 2 or 3. (Later in this section, we prove that this  
 12 graph cannot be reduced to an edge even if we allow “backward” facial electrical transformations that  
 13 make the graph more complicated.)

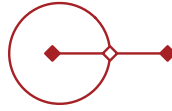


Figure 3.1. A facially irreducible 2-terminal plane graph.

14 In this section, we show that in the worst case,  $\Omega(n^2)$  facial electrical transformations are required  
 15 to reduce an 2-terminal plane graph with  $n$  vertices *as much as possible*. First, we prove in Section 3.1  
 16 that any 2-terminal planar graph can be reduced to a unique minimal graph called a *bullseye* by facial  
 17 electrical transformations. We prove our quadratic lower bound in Section 3.2.

18 Existing algorithms for reducing an arbitrary 2-terminal plane graphs to a single edge rely on an addi-  
 19 tional operation which we call a *terminal-leaf contraction*, in addition to facial electrical transformations.  
 20 We discuss this subtlety in more detail in Section 3.3.

### 21 3.1 Winding Number, Medial Depth, and Bullseyes

22 The medial graph  $G^\times$  of any 2-terminal plane graph  $G$  is properly considered as a multicurve embedded  
 23 in the annulus; the faces of  $G^\times$  that correspond to the terminals are removed from the surface.

24 The *winding number* of a directed closed curve  $\gamma$  in the annulus is the number of times any generic  
 25 path  $\alpha$  from one boundary component to the other crosses  $\gamma$  from left to right, minus the number of  
 26 times  $\alpha$  crosses  $\gamma$  from right to left. Two directed closed curves in the annulus are homotopic if and only  
 27 if their winding numbers are equal.

28 The *depth* of any multicurve  $\gamma$  in the annulus is the minimum number of times a path from one  
 29 boundary to the other crosses  $\gamma$ ; thus, depth is essentially an unsigned version of winding number.  
 30 Just as the winding number around the boundaries is a complete homotopy invariant for curves in  
 31 the annulus, the depth of the medial graph turns out to be a complete invariant for facial electrical  
 32 transformation of 2-terminal plane graphs.

33 **Lemma 3.1.** *Medial electrical transformations do not change the depth of any connected multicurve in*  
 34 *the annulus. Thus, facial electrical transformations in any 2-terminal plane graph  $G$  do not change the*  
 35 *depth of the medial graph  $G^\times$ .*

36 **Proof:** Let  $\gamma$  be a connected multicurve in the annulus. For any face of  $\gamma$  that could be deleted by a  
 37 medial electrical move, exhaustive case analysis implies that there is a shortest path between the two  
 38 boundary faces of  $\gamma$  that avoids that face. □

1 For any integer  $d > 0$ , let  $\alpha_d$  denote the unique closed curve in the annulus with  $d - 1$  vertices and  
 2 winding number  $d$ . Up to isotopy, this curve can be parametrized in the plane as

$$3 \quad \alpha_d(\theta) := ((\cos(\theta) + 2) \cos(d\theta), (\cos(\theta) + 2) \sin(d\theta)).$$

4 In the notation of our other papers [8, 9],  $\alpha_d$  is the *flat torus knot*  $T(d, 1)$ .

5 Similarly, for any  $k > 0$ , let  $B_k$  denote the 2-terminal plane graph that consists of a path of length  $k$   
 6 between the terminals, with a loop attached to each of the  $k - 1$  interior vertices, embedded so that  
 7 collectively they form concentric circles that separate the terminals. We call each graph  $B_k$  a **bullseye**.  
 8 For example,  $B_1$  is just a single edge;  $B_2$  is shown in Figure 3.1; and  $B_4$  is shown on the left in Figure 3.2.  
 9 The medial graph  $B_k^\times$  of the  $k$ th bullseye is the curve  $\alpha_{2k}$ . Because different bullseyes have different  
 10 medial depths, Lemma 3.1 implies that no bullseye can be transformed into any other bullseye by facial  
 11 electrical transformations.

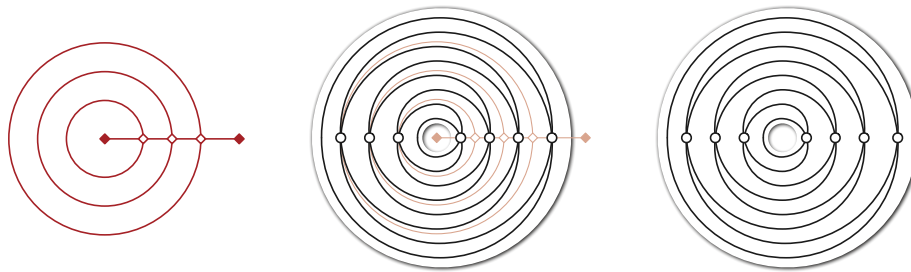


Figure 3.2. The bullseye graph  $B_4$  and its medial graph  $\alpha_8$ .

12 **Lemma 3.2.** For any integer  $d > 0$ , the curve  $\alpha_d$  is both homotopically reduced and electrically reduced.

13 **Proof:** Every connected multicurve in the annulus with either winding number  $d$  or depth  $d$  has at least  
 14  $d + 1$  faces (including the faces containing the boundaries of the annulus) and therefore, by Euler's  
 15 formula, has at least  $d - 1$  vertices.  $\square$

16 **Lemma 3.3.** If  $\gamma$  is a homotopically reduced connected multicurve in the annulus, then  $\gamma = \alpha_d$  for some  
 17 integer  $d$ .

18 **Proof:** A multicurve in the annulus is homotopically reduced if and only if its constituent curves are  
 19 homotopically reduced and disjoint. Thus, any connected homotopically reduced multicurve is actually a  
 20 single closed curve. Any two curves in the annulus with the same winding number are homotopic [24].  
 21 Finally, up to isotopy,  $\alpha_d$  is the only closed curve in the annulus with winding number  $d$  and  $d - 1$   
 22 vertices [22, Lemma 1.12].  $\square$

23 **Lemma 3.4.** Let  $\gamma$  be a connected multicurve on any surface, possibly with boundary. If  $\gamma$  is electrically  
 24 reduced, then  $\gamma$  is also homotopically reduced.

25 **Proof:** Let  $\gamma$  be a connected multicurve in some arbitrary surface, and suppose  $\gamma$  is not homotopically  
 26 reduced. A seminal result of de Graaf and Schrijver [21] implies that  $\gamma$  can be simplified by a finite  
 27 sequence of homotopy moves<sup>1</sup> that never increases the number of vertices. In particular, applying  
 28 some finite sequence of 3→3 moves to  $\gamma$  creates either an empty loop, which can be removed by a 1→0  
 29 move, or an empty bigon, which can be removed by either a 2→0 move or a 2→1 move. Thus,  $\gamma$  is not  
 30 electrically reduced.  $\square$

<sup>1</sup>De Graaf and Schrijver's result requires a fourth type of homotopy move, which moves an isolated simple contractible constituent curve from one face of the rest of the multicurve to another. However, since this move can only be applied to disconnected multicurves, it does not affect our argument.

The following corollaries are now immediate.

**Corollary 3.5.** *A connected multicurve  $\gamma$  in the annulus is electrically reduced if and only if  $\gamma = \alpha_{\text{depth}(\gamma)}$ .*

**Corollary 3.6.** *Let  $\gamma$  and  $\gamma'$  be two connected multicurves in the annulus. Then  $\gamma$  can be transformed into  $\gamma'$  by medial electrical moves if and only if  $\text{depth}(\gamma) = \text{depth}(\gamma')$ .*

**Corollary 3.7.** *Let  $G$  be an arbitrary 2-terminal plane graph.  $G$  can be reduced to the bullseye  $B_k$  using a finite sequence of facial electrical transformations if and only if  $\text{depth}(G^\times) = 2k$ .*

**Corollary 3.8.** *Let  $G$  and  $H$  be arbitrary 2-terminal plane graphs.  $G$  can be transformed to  $H$  using a finite sequence of facial electrical transformations if and only if  $\text{depth}(G^\times) = \text{depth}(H^\times)$ .*

### 3.2 Quadratic Lower Bound

For any connected multicurve  $\gamma$ , let  $X(\gamma)$  denote the minimum number of medial electrical moves required to reduce  $\gamma$  as much as possible, and let  $H(\gamma)$  denote the minimum number of homotopy moves required to reduce  $\gamma$  as much as possible. Our quadratic lower bound proof generally follows our earlier proof that  $X(\gamma) \geq H(\gamma)$  for any closed curve  $\gamma$  in the plane or the sphere [8, Lemma 3.3], which is based in turn on arguments of Truemper [33] and Noble and Welsh [27].

**Lemma 3.9.** *For any connected proper smoothing  $\bar{\gamma}$  of any connected multicurve  $\gamma$  in the annulus, we have  $X(\bar{\gamma}) + \frac{1}{2} \text{depth}(\bar{\gamma}) \leq X(\gamma) + \frac{1}{2} \text{depth}(\gamma)$ .*

**Proof:** Let  $\gamma$  be an arbitrary connected multicurve in the annulus, and let  $\bar{\gamma}$  be an arbitrary connected proper smoothing of  $\gamma$ . Without loss of generality, we can assume that  $\gamma$  is non-simple, since otherwise the lemma is vacuous.

First, suppose  $\bar{\gamma}$  is a connected smoothing of  $\gamma$  obtained by smoothing a single vertex  $x$ . There are only two cases to consider: Either  $\gamma$  is electrically reduced or not.

If  $\gamma$  is electrically reduced, then  $\gamma = \alpha_d$  for some integer  $d \geq 2$  by Corollary 3.5. (The curves  $\alpha_0$  and  $\alpha_1$  are simple.) The smoothed curve  $\bar{\gamma}$  contains a single loop if  $x$  is the innermost or outermost vertex of  $\gamma$ , or a single bigon otherwise. Applying one  $1 \rightarrow 0$  or  $2 \rightarrow 0$  move transforms  $\bar{\gamma}$  into the curve  $\alpha_{d-2}$ , which is electrically reduced by Lemma 3.2. Thus we have  $X(\bar{\gamma}) = 1$  and  $\text{depth}(\bar{\gamma}) = d - 2$ , which implies  $X(\bar{\gamma}) + \frac{1}{2} \text{depth}(\bar{\gamma}) = X(\gamma) + \frac{1}{2} \text{depth}(\gamma)$ .

On the other hand, suppose  $\gamma$  is not reduced. We argue by induction on  $X(\gamma)$ , with the set of reduced curves as a base case, closely following our earlier proof [8, Lemma 3.1]. Let  $\gamma'$  be the result of the first medial electrical move in the minimum-length sequence that reduces  $\gamma$ . We immediately have  $X(\gamma') = X(\gamma) - 1$  and  $\text{depth}(\gamma') = \text{depth}(\gamma)$ . There are several subcases to consider, depending on whether the move from  $\gamma$  to  $\gamma'$  involves the smoothed vertex  $x$ , and if so, on the type of move and how  $x$  is smoothed. In all cases, there is a connected multicurve  $\bar{\gamma}'$  that can be obtained both by applying at most one medial electrical move to  $\bar{\gamma}$  and by smoothing at most two vertices of  $\gamma'$ .

Specifically, if the move from  $\gamma$  to  $\gamma'$  does not involve  $x$ , we can define  $\bar{\gamma}' = \bar{\gamma}$ ; the remaining eight subcases are illustrated in Figure 3.3. One subcase for the  $0 \rightarrow 1$  move is impossible, because we have assumed that  $\bar{\gamma}$  is connected. In the remaining  $0 \rightarrow 1$  subcase and one  $2 \rightarrow 1$  subcase, we can define  $\bar{\gamma}' = \bar{\gamma} = \gamma'$ , and in all remaining subcases,  $\bar{\gamma}'$  is a proper smoothing of  $\gamma'$ .

In every case, we have  $\text{depth}(\gamma) = \text{depth}(\gamma')$  and  $\text{depth}(\bar{\gamma}) = \text{depth}(\bar{\gamma}')$ , and therefore

$$\begin{aligned} X(\bar{\gamma}) + \frac{1}{2} \text{depth}(\bar{\gamma}) &\leq X(\bar{\gamma}') + 1 + \frac{1}{2} \text{depth}(\bar{\gamma}') \\ &\leq X(\gamma') + 1 + \frac{1}{2} \text{depth}(\gamma') \\ &\leq X(\gamma) + \frac{1}{2} \text{depth}(\gamma), \end{aligned} \tag{*}$$

1 where the second inequality (\*) is either trivial (because  $\bar{\gamma}' = \gamma'$ ) or follows from the induction hypothesis  
 2 (because  $\bar{\gamma}'$  is a proper smoothing of  $\gamma'$ ).

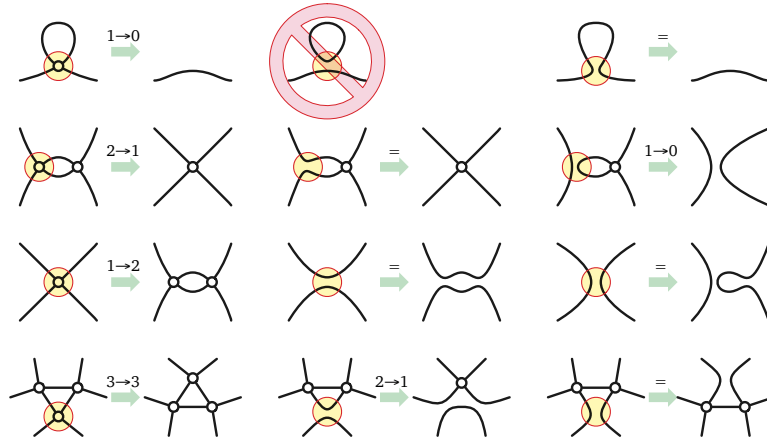


**Figure 3.3.** Cases for the proofs of Lemma 3.9 and 4.6; the circled vertex is  $x$ .

3 Finally, if  $\bar{\gamma}$  is obtained from  $\gamma$  by smoothing more than one vertex, the lemma follows from the  
 4 previous cases by induction on the number of vertices. □

5 **Lemma 3.10.** *For every connected multicurve  $\gamma$  in the annulus, there is a minimum-length sequence of*  
 6 *medial electrical moves that reduces  $\gamma$  to  $\alpha_{\text{depth}(\gamma)}$  without  $0 \rightarrow 1$  or  $1 \rightarrow 2$  moves.*

7 **Proof:** Consider a minimum-length sequence of medial electrical moves that reduces an arbitrary  
 8 connected multicurve  $\gamma$  in the annulus. For any integer  $i \geq 0$ , let  $\gamma_i$  denote the result of the first  $i$  moves  
 9 in this sequence. Suppose  $\gamma_i$  has one more vertex than  $\gamma_{i-1}$  for some index  $i$ . Then  $\gamma_{i-1}$  is a connected  
 10 proper smoothing of  $\gamma_i$ , and  $\text{depth}(\gamma_i) = \text{depth}(\gamma_{i-1})$ ; so Lemma 3.9 implies that  $X(\gamma_{i-1}) \leq X(\gamma_i)$ ,  
 11 contradicting our assumption that the reduction sequence has minimum length. □

12 **Lemma 3.11.**  $X(\gamma) + \frac{1}{2} \text{depth}(\gamma) \geq H(\gamma)$  for every closed curve  $\gamma$  in the annulus.

13 **Proof:** Let  $\gamma$  be a closed curve in the annulus. If  $\gamma$  is already electrically reduced, then  $X(\gamma) = H(\gamma) = 0$   
 14 by Lemma 3.4, so the lemma is trivial. Otherwise, let  $\Sigma$  be a minimum-length sequence of medial  
 15 electrical moves that reduces  $\gamma$  as much as possible. By Lemma 3.10, we can assume that the first move  
 16 in  $\Sigma$  is neither  $0 \rightarrow 1$  nor  $1 \rightarrow 2$ . If the first move is  $1 \rightarrow 0$  or  $3 \rightarrow 3$ , the theorem immediately follows by  
 17 induction on  $X(\gamma)$ , since by Lemma 3.1 neither of these moves changes the depth of the curve.

18 The only interesting first move is  $2 \rightarrow 1$ . Let  $\gamma'$  be the result of this  $2 \rightarrow 1$  move, and let  $\gamma^\circ$  be the  
 19 result if we perform the  $2 \rightarrow 0$  homotopy move on the same vertex instead. The minimality of  $\Sigma$  implies  
 20  $X(\gamma) = X(\gamma') + 1$ , and we trivially have  $H(\gamma) \leq H(\gamma^\circ) + 1$ . Because  $\gamma$  is a single curve,  $\gamma^\circ$  is also a single  
 21 curve and therefore a connected proper smoothing of  $\gamma'$ . Thus, Lemmas 3.1 and 3.9 and the inductive  
 22 hypothesis imply

$$\begin{aligned}
 23 \quad X(\gamma) + \frac{1}{2} \text{depth}(\gamma) &= X(\gamma') + \frac{1}{2} \text{depth}(\gamma') + 1 \\
 24 &\geq X(\gamma^\circ) + \frac{1}{2} \text{depth}(\gamma^\circ) + 1 \\
 25 &\geq H(\gamma^\circ) + 1 \\
 26 &\geq H(\gamma), \\
 27
 \end{aligned}$$

28 which completes the proof. □

**Theorem 3.12.** *Let  $G$  be an arbitrary 2-terminal plane graph, and let  $\gamma$  be any unicursal smoothing of  $G^\times$ . Reducing  $G$  to a bullseye requires at least  $H(\gamma) - \frac{1}{2} \text{depth}(\gamma)$  facial electrical transformations.*

In a companion paper [10], we describe an infinite family of contractible curves in the annulus that require  $\Omega(n^2)$  homotopy moves to simplify. Because these curves are contractible, they have even depth, and thus are the medial graphs of 2-terminal plane graphs. Euler’s formula implies that every  $n$ -vertex curve in the annulus has exactly  $n + 2$  faces (including the boundary faces) and therefore has depth at most  $n + 1$ .

**Corollary 3.13.** *Reducing a 2-terminal plane graph to a bullseye requires  $\Omega(n^2)$  facial electrical transformations in the worst case.*

### 3.3 Terminal-Leaf Contractions

The electrical reduction algorithms of Feo [17], Truemper [33], and Feo and Provan [18] rely exclusively on facial electrical transformations, plus one additional operation.

- *Terminal-leaf contraction:* Contract the edge incident to a *terminal* vertex with degree 1. The neighbor of the deleted terminal becomes a new terminal.

Terminal-leaf contractions are also called *FP-assignments*, after Feo and Provan [12, 19, 20]. Later algorithms for reducing plane graphs with three or four terminals [3, 12, 20] also use only facial electrical transformations and terminal-leaf contractions.

Formally, terminal-leaf contractions are *not* electrical transformations, as they can change the value one wants to compute. For example, if the edges in the graph shown in Figure 3.1 represent  $1\Omega$  resistors, a terminal-leaf contraction changes the effective resistance between the terminals from  $2\Omega$  to  $1\Omega$ . However, both Gilter [19] and Feo and Provan [18] observed that any sequence of facial electrical transformations and terminal-leaf contractions can be simulated on the fly by a sequence of *planar* electrical transformations. Specifically, we simulate the first leaf contraction at either terminal by simply marking that terminal and proceeding as if its unique neighbor were a terminal. Later electrical transformations involving the neighbor of a marked terminal may no longer be facial, but they will still be planar; terminal-leaf contractions at the unique neighbor of a marked terminal become series reductions. At the end of the sequence of transformations, we perform a final series reduction at the unique neighbor of each marked terminal.

Unfortunately, terminal-leaf contractions change both the depth of the medial graph and the curve invariants that imply the quadratic homotopy lower bound. As a result, our quadratic lower bound proof breaks down if we allow terminal-leaf contractions. Indeed, we conjecture that any 2-terminal plane graph can be reduced to a single edge using only  $O(n^{3/2})$  facial electrical transformations and terminal-leaf contractions, matching the lower bound proved in Section 4.

## 4 Planar Electrical Transformations

Finally, we extend our earlier  $\Omega(n^{3/2})$  lower bound for reducing plane graphs *without* terminals using only facial electrical transformations to the larger class of planar electrical transformations. As in our earlier work [8], we analyze electrical transformations in an unicursal plane graph  $G$  in terms of a certain invariant of the medial graph of  $G$  called *defect*, first introduced by Aicardi [2] and Arnold [4, 5]. Our extension to non-facial electrical transformations is based on the following surprising observation: Although the medial graph of  $G$  depends on its embedding, the *defect* of the medial graph of  $G$  does not.

## 4.1 Defect

Let  $\gamma$  be an arbitrary closed curve on the sphere. Choose an arbitrary basepoint  $\gamma(0)$  and an arbitrary orientation for  $\gamma$ . For any vertex  $x$  of  $\gamma$ , we define  $\text{sgn}(x) = +1$  if the first traversal through  $x$  crosses the second traversal from right to left, and  $\text{sgn}(x) = -1$  otherwise. Two vertices  $x$  and  $y$  are *interleaved*, denoted  $x \bowtie y$ , if they alternate in cyclic order— $x, y, x, y$ —along  $\gamma$ . Finally, following Polyak [28], we can define

$$\text{defect}(\gamma) := -2 \sum_{x \bowtie y} \text{sgn}(x) \cdot \text{sgn}(y),$$

where the sum is taken over all interleaved pairs of vertices of  $\gamma$ .

Trivially, every simple closed curve has defect zero. Straightforward case analysis [28] implies that the defect of a curve does not depend on the choice of basepoint or orientation. Moreover, any homotopy move changes the defect of a curve by at most 2; see our previous paper [8, Section 2.1] for an explicit case breakdown. Defect is also preserved by any homeomorphism from the sphere to itself, including reflection.

## 4.2 Tangle Flips

Now let  $\sigma$  be a simple closed curve that intersects  $\gamma$  only transversely and away from its vertices. By the Jordan curve theorem, we can assume without loss of generality that  $\sigma$  is a circle, and that the intersection points  $\gamma \cap \sigma$  are evenly spaced around  $\sigma$ . A *tangle* of  $\gamma$  is the intersection of  $\gamma$  with either disk bounded by  $\sigma$ ; each tangle consists of one or more subpaths of  $\gamma$  called *strands*. We arbitrarily refer to the two tangles defined by  $\sigma$  as the *interior* and *exterior* tangles of  $\sigma$ .

A tangle is *tight* if each strand is simple and each pair of strands crosses at most once. Any tangle can be *tightened*—that is, transformed into a tight tangle—by continuously deforming the strands without crossing  $\sigma$  or moving their endpoints, and therefore by a finite sequence of homotopy moves. Let  $\gamma \pitchfork \sigma$  and  $\gamma \cup \sigma$  denote the closed curves that result from tightening the interior and exterior tangles of  $\sigma$ , respectively.<sup>2</sup>



Figure 4.1. Flipping tangles with one and two strands.

Finally, we can *flip* any tangle by reflecting the disk containing it, so that each strand endpoint maps to a different strand endpoint; see Figure 4.1. Straightforward case analysis implies that flipping any tangle of  $\gamma$  with at most two strands transforms  $\gamma$  into another closed curve. The main result of this section is that the resulting curve has the same defect as  $\gamma$ .

**Lemma 4.1.** *Let  $\gamma$  be an arbitrary closed curve on the sphere. Flipping any tangle of  $\gamma$  with one strand yields another closed curve  $\gamma'$  with  $\text{defect}(\gamma') = \text{defect}(\gamma)$ .*

**Proof:** Let  $\sigma$  be a simple closed curve that crosses  $\gamma$  at exactly two points. These points decompose  $\sigma$  into two subpaths  $\alpha \cdot \beta$ , where  $\alpha$  is the unique strand of the interior tangle and  $\beta$  is the unique strand of the exterior tangle. Let  $\Sigma$  denote the interior disk of  $\sigma$ , and let  $\phi : \Sigma \rightarrow \Sigma$  denote the homeomorphism that flips the interior tangle. Flipping the interior tangle yields the closed curve  $\gamma' := \text{rev}(\phi(\alpha)) \cdot \beta$ , where *rev* denotes path reversal.

<sup>2</sup>We recommend pronouncing  $\pitchfork$  as “tightened inside” and  $\cup$  as “tightened outside”; note that the symbols  $\pitchfork$  and  $\cup$  resemble the second letters of “inside” and “outside”.

1 No vertex of  $\alpha$  is interleaved with a vertex of  $\beta$ ; thus, two vertices in  $\gamma'$  are interleaved if and only  
 2 if the corresponding vertices in  $\gamma$  are interleaved. Every vertex of  $\text{rev}(\phi(\alpha))$  has the same sign as the  
 3 corresponding vertex of  $\alpha$ , since both the orientation of the vertex and the order of traversals through  
 4 the vertex changed. Thus, every vertex of  $\gamma'$  has the same sign as the corresponding vertex of  $\gamma$ . We  
 5 conclude that  $\text{defect}(\gamma') = \text{defect}(\gamma)$ .  $\square$

6 **Lemma 4.2.** *Let  $\gamma$  be an arbitrary closed curve on the sphere. Flipping any tangle of  $\gamma$  with two strands*  
 7 *yields another closed curve  $\gamma'$  with  $\text{defect}(\gamma') = \text{defect}(\gamma)$ .*

8 **Proof:** Let  $\sigma$  be a simple closed curve that crosses  $\gamma$  at exactly four points. These four points naturally  
 9 decompose  $\gamma$  into four subpaths  $\alpha \cdot \delta \cdot \beta \cdot \varepsilon$ , where  $\alpha$  and  $\beta$  are the strands of the interior tangle of  $\sigma$ ,  
 10 and  $\delta$  and  $\varepsilon$  are the strands of the exterior tangle. Flipping the interior tangle either exchanges  $\alpha$  and  $\beta$ ,  
 11 reverses  $\alpha$  and  $\beta$ , or both; see Figure 4.2. In every case, the result is a single closed curve  $\gamma'$ .

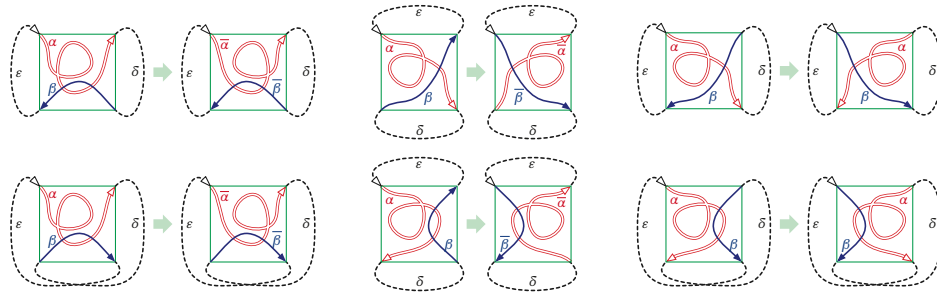


Figure 4.2. Flipping all six types of 2-strand tangle.

12 The identity  $\text{defect}(\gamma') = \text{defect}(\gamma)$  follows from our inclusion-exclusion formula for defect [7,  
 13 Lemma 5.4]; we give a simpler complete proof here to keep the paper self-contained.

14 We classify each vertex of  $\gamma$  as *interior* if it lies on  $\alpha$  and/or  $\beta$ , and *exterior* otherwise. Similarly, we  
 15 classify pairs of interleaved vertices are either interior, exterior, or mixed.

16 An interior vertex  $x$  and an exterior vertex  $y$  are interleaved if and only if  $x$  is an intersection point  
 17 of  $\alpha$  and  $\beta$  and  $y$  is an intersection point of  $\delta$  and  $\varepsilon$ . Thus, the total contribution of mixed vertex pairs  
 18 to Polyak's formula  $\text{defect}(\gamma) = -2 \sum_{x \not\parallel y} \text{sgn}(x) \cdot \text{sgn}(y)$  is

$$-2 \sum_{x \in \alpha \cap \beta} \sum_{y \in \delta \cap \varepsilon} \text{sgn}(x) \cdot \text{sgn}(y) = -2 \left( \sum_{x \in \alpha \cap \beta} \text{sgn}(x) \right) \left( \sum_{y \in \delta \cap \varepsilon} \text{sgn}(y) \right).$$

20 Consider any sequence of homotopy moves that tightens the interior tangle with strands  $\alpha$  and  $\beta$ . Any  
 21  $2 \rightarrow 0$  move involving both  $\alpha$  and  $\beta$  removes one positive and one negative vertex; no other homotopy  
 22 move changes the number of vertices in  $\alpha \cap \beta$  or the signs of those vertices. Thus, tightening  $\alpha$  and  $\beta$   
 23 leaves the sum  $\sum_{x \in \alpha \cap \beta} \text{sgn}(x)$  unchanged. Similarly, tightening the exterior tangle  $\delta \cup \varepsilon$  leaves the sum  
 24  $\sum_{y \in \delta \cap \varepsilon} \text{sgn}(y)$  unchanged. But after tightening both tangles, either  $\alpha$  and  $\beta$  are disjoint, or  $\delta$  and  $\varepsilon$   
 25 are disjoint, or both, as  $\gamma$  is a single closed curve. Thus, at least one of the sums  $\sum_{x \in \alpha \cap \beta} \text{sgn}(x)$  and  
 26  $\sum_{y \in \delta \cap \varepsilon} \text{sgn}(y)$  is equal to zero. We conclude that mixed vertex pairs do not contribute to the defect.

27 The curve  $\gamma \pitchfork \sigma$  obtained by tightening  $\alpha$  and  $\beta$  has at most one interior vertex (and therefore no  
 28 interior vertex pairs); the exterior vertices of  $\gamma \pitchfork \sigma$  are precisely the exterior vertices of  $\gamma$ . Similarly, the  
 29 curve  $\gamma \cup \sigma$  obtained by tightening both  $\delta$  and  $\varepsilon$  has at most one exterior vertex; the interior vertices of  
 30  $\gamma \cup \sigma$  are precisely the interior vertices of  $\gamma$ . It follows that  $\text{defect}(\gamma) = \text{defect}(\gamma \cup \sigma) + \text{defect}(\gamma \pitchfork \sigma)$ .

1 Finally, let  $\gamma'$  be the result of flipping the interior tangle. The curve  $\gamma' \cup \sigma$  is just a reflection of  $\gamma \cup \sigma$ ,  
 2 which implies that  $\text{defect}(\gamma' \cup \sigma) = \text{defect}(\gamma \cup \sigma)$ , and straightforward case analysis implies  $\gamma' \cap \sigma = \gamma \cap \sigma$ .  
 3 We conclude that  $\text{defect}(\gamma') = \text{defect}(\gamma' \cap \sigma) + \text{defect}(\gamma' \cup \sigma) = \text{defect}(\gamma \cap \sigma) + \text{defect}(\gamma \cup \sigma) = \text{defect}(\gamma)$ .  $\square$

### 4.3 Navigating Between Planar Embeddings

4 A classical result of Adkisson [1] and Whitney [36] is that every 3-connected planar graph has an  
 5 essentially unique planar embedding. Mac Lane [26] described how to count the planar embeddings of  
 6 any biconnected planar graph, by decomposing it into its triconnected components. Stallmann [29,30]  
 7 and Cai [6] extended Mac Lane’s algorithm to arbitrary planar graphs, by decomposing them into  
 8 biconnected components. Mac Lane’s decomposition is also the basis of the SPQR-tree data structure of  
 9 Di Battista and Tamassia [13, 14], which encodes all planar embeddings of an arbitrary planar graph.  
 10

11 Mac Lane’s structural results imply that any planar embedding of a 2-connected planar graph  $G$  can  
 12 be transformed into any other embedding by a finite sequence of **split reflections**, defined as follows.  
 13 A **split curve** is a simple closed curve  $\sigma$  whose intersection with the embedding of  $G$  consists of two  
 14 vertices  $x$  and  $y$ ; without loss of generality,  $\sigma$  is a circle with  $x$  and  $y$  at opposite points. A split reflection  
 15 modifies the embedding of  $G$  by reflecting the subgraph inside  $\sigma$  across the line through  $x$  and  $y$ .

16 **Lemma 4.3.** *Let  $G$  be an arbitrary 2-connected planar graph. Any planar embedding of  $G$  can be*  
 17 *transformed into any other planar embedding of  $G$  by a finite sequence of split reflections.*

18 To navigate among the planar embeddings of *arbitrary* connected planar graphs, we need two  
 19 additional operations. First, we allow split curves that intersect  $G$  at only a single cut vertex; a **cut**  
 20 **reflection** modifies the embedding of  $G$  by reflects the subgraph inside such a curve. More interestingly,  
 21 we also allow degenerate split curves that pass through a cut vertex  $x$  of  $G$  *twice*, but are otherwise  
 22 simple and disjoint from  $G$ . The interior of a degenerate split curve  $\sigma$  is an open topological disk. A  
 23 **cut eversion** is a degenerate split reflection that everts the embedding of the subgraph of  $G$  inside such  
 24 a curve, intuitively by mapping the interior of  $\sigma$  to an open circular disk (with two copies of  $x$  on its  
 25 boundary), reflecting the interior subgraph, and then mapping the resulting embedding back to the  
 26 interior of  $\sigma$ . Structural results of Stallman [29,30] and Di Battista and Tamassia [14, Section 7] imply  
 27 the following.

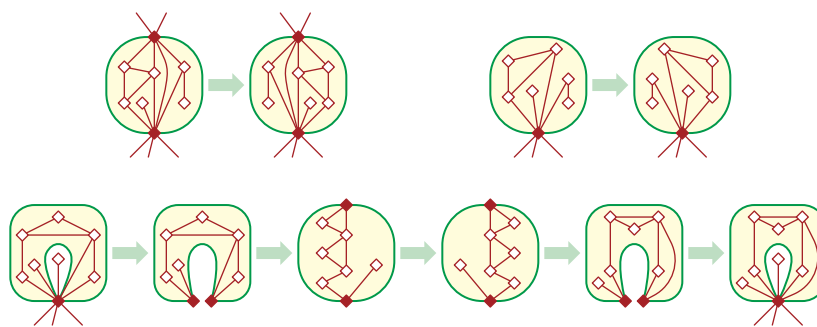


**Figure 4.3.** Top row: A regular split reflection and a cut reflection. Bottom row: a cut eversion.

28 **Lemma 4.4.** *Let  $G$  be an arbitrary connected planar graph. Any planar embedding of  $G$  can be*  
 29 *transformed into any other planar embedding of  $G$  by a finite sequence of split reflections, cut reflections,*  
 30 *and cut eversions.*

31 Now consider the effect of these operations on the medial graph  $G^\times$ . For simplicity, assume  $G^\times$  is a  
 32 single closed curve. Let  $\sigma$  be any (possibly degenerate) split curve for  $G$ . Embed  $G^\times$  so that every medial

vertex lies on the corresponding edge in  $G$ , and every medial edge intersects  $\sigma$  at most once. Then  $\sigma$  intersects at most four edges of  $G^\times$ , so the tangle of  $G^\times$  inside  $\sigma$  has at most two strands. Moreover, reflecting (or everting) the subgraph of  $G$  inside  $\sigma$  induces a flip of this tangle of  $G^\times$ .

Lemmas 4.1, 4.2, and 4.4 now immediately imply the following result.

**Theorem 4.5.** *Let  $G$  and  $H$  be planar embeddings of the same abstract planar graph. If  $G$  is unicursal, then  $H$  is unicursal and  $\text{defect}(G^\times) = \text{defect}(H^\times)$ .*

#### 4.4 Back to Planar Electrical Moves

Each planar electrical transformation in a planar graph  $G$  induces the same change in the medial graph  $G^\times$  as a finite sequence of 1- and 2-strand tangle flips (hereafter simply called “tangle flips”) followed by a single medial electrical move. For an arbitrary connected multicurve  $\gamma$  on the sphere, let  $\bar{X}(\gamma)$  denote the minimum number of medial electrical moves in a mixed sequence of medial electrical moves and tangle flips that simplifies  $\gamma$ . Similarly, let  $\bar{H}(\gamma)$  denote the minimum number of homotopy moves in a mixed sequence of homotopy moves and tangle flips that simplifies  $\gamma$ . We emphasize that tangle flips are “free” and do not contribute to either  $\bar{X}(\gamma)$  or  $\bar{H}(\gamma)$ .

Our lower bound on planar electrical moves follows our earlier lower bound proof for facial electrical moves [8] almost verbatim; the only subtlety is that the embedding of the graph can effectively change at every step of the reduction. We repeat the arguments here to keep the paper self-contained.

**Lemma 4.6.**  *$\bar{X}(\bar{\gamma}) < \bar{X}(\gamma)$  for every connected proper smoothing  $\bar{\gamma}$  of every connected multicurve  $\gamma$  on the sphere.*

**Proof:** Let  $\gamma$  be a connected multicurve, and let  $\bar{\gamma}$  be a connected proper smoothing of  $\gamma$ . The proof proceeds by induction on  $\bar{X}(\gamma)$ . If  $\bar{X}(\gamma) = 0$ , then  $\gamma$  is already simple, so the lemma is vacuously true.

First, suppose  $\bar{\gamma}$  is obtained from  $\gamma$  by smoothing a single vertex  $x$ . Let  $\Sigma$  be an optimal mixed sequence of tangle flips and medial electrical moves that simplifies  $\gamma$ . This sequence starts with zero or more tangle flips, followed by a medial electrical move. Let  $\gamma'$  be the multicurve that results from the initial sequence of tangle flips; by definition, we have  $\bar{X}(\gamma) = \bar{X}(\gamma')$ . Moreover, applying the same sequence of tangle flips to  $\bar{\gamma}$  yields a connected multicurve  $\bar{\gamma}'$  such that  $\bar{X}(\bar{\gamma}) = \bar{X}(\bar{\gamma}')$ . Thus, we can assume without loss of generality that the first operation in  $\Sigma$  is a medial electrical move.

Now let  $\gamma'$  be the result of this move; by definition, we have  $\bar{X}(\gamma) = \bar{X}(\gamma') + 1$ . As in the proof of Lemma 3.9, there are several subcases to consider, depending on whether the move from  $\gamma$  to  $\gamma'$  involves the smoothed vertex  $x$ , and if so, the specific type of move; see Figure 3.3. In every subcase, we can apply at most one medial electrical move to  $\bar{\gamma}$  to obtain a (possibly trivial) smoothing  $\bar{\gamma}'$  of  $\gamma'$ , and then apply the inductive hypothesis on  $\gamma'$  and  $\bar{\gamma}'$  to prove the statement. We omit the straightforward details.

Finally, if  $\bar{\gamma}$  is obtained from  $\gamma$  by smoothing more than one vertex, the lemma follows immediately by induction from the previous analysis.  $\square$

**Lemma 4.7.** *For every connected multicurve  $\gamma$ , there is an intermixed sequence of medial electrical moves and tangle flips that reduces  $\gamma$  to a simple closed curve, contains exactly  $\bar{X}(\gamma)$  medial electrical moves, and does not contain  $0 \rightarrow 1$  or  $1 \rightarrow 2$  moves.*

**Proof:** Consider an optimal sequence of medial electrical moves and tangle flips that reduces  $\gamma$ , and let  $\gamma_i$  denote the result of the first  $i$  moves in this sequence. If any  $\gamma_i$  has more vertices than its predecessor  $\gamma_{i-1}$ , then  $\gamma_{i-1}$  is a connected proper smoothing of  $\gamma_i$ , and Lemma 4.6 implies a contradiction.  $\square$

**Lemma 4.8.**  *$\bar{X}(\gamma) \geq \bar{H}(\gamma)$  for every closed curve  $\gamma$  on the sphere.*

**Proof:** Let  $\gamma$  be a planar closed curve. The proof proceeds by induction on  $\bar{X}(\gamma)$ . If  $\bar{X}(\gamma) = 0$ , then  $\gamma$  is simple and thus  $\bar{H}(\gamma) = 0$ , so assume otherwise.

Let  $\Sigma$  be an optimal sequence of medial electrical moves and tangle flips that reduces  $\gamma$ , and let  $\gamma_i$  be the curve obtained by applying a prefix of  $\Sigma$  up to and including the first medial electrical move. The minimality of  $\Sigma$  implies that  $\bar{X}(\gamma) = \bar{X}(\gamma') + 1$ . By Lemma 4.7, we can assume without loss of generality that the first medial electrical move in  $\Sigma$  is neither  $0 \rightarrow 1$  nor  $1 \rightarrow 2$ , and if this first medial electrical move is  $1 \rightarrow 0$  or  $3 \rightarrow 3$ , the theorem immediately follows by induction.

The only remaining move to consider is  $2 \rightarrow 1$ . Let  $\bar{\gamma}$  denote the result of applying the same sequence of tangle flips to  $\gamma$ , but replacing the final  $2 \rightarrow 1$  move with a  $2 \rightarrow 0$  move, or equivalently, smoothing the vertex of  $\gamma'$  left by the final  $2 \rightarrow 1$  move. We immediately have  $\bar{H}(\gamma) \leq \bar{H}(\bar{\gamma}) + 1$ . Because  $\bar{\gamma}$  is a connected proper smoothing of  $\gamma'$ , Lemma 4.6 implies  $\bar{X}(\bar{\gamma}) < \bar{X}(\gamma') = \bar{X}(\gamma) - 1$ . Finally, the inductive hypothesis implies that  $\bar{X}(\bar{\gamma}) \geq \bar{H}(\bar{\gamma})$ , which completes the proof.  $\square$

**Lemma 4.9.**  $\bar{H}(\gamma) \geq |\text{defect}(\gamma)|/2$  for every closed curve  $\gamma$  on the sphere.

**Proof:** Each homotopy move decreases  $|\text{defect}(\gamma)|$  by at most 2, and Lemmas 4.1 and 4.2 imply that tangle flips do not change  $|\text{defect}(\gamma)|$  at all. Every simple curve has defect 0.  $\square$

**Theorem 4.10.** Let  $G$  be an arbitrary planar graph, and let  $\gamma$  be any unicursal smoothing of  $G^\times$  (defined with respect to any planar embedding of  $G$ ). Reducing  $G$  to a single vertex requires at least  $|\text{defect}(\gamma)|/2$  planar electrical transformations.

**Proof:** The minimum number of planar electrical transformations required to reduce  $G$  is at least  $\bar{X}(G^\times)$ . Because  $\gamma$  is a single curve, it must be connected, so Lemma 4.6 implies that  $\bar{X}(G^\times) \geq \bar{X}(\gamma)$ . The theorem now follows immediately from Lemmas 4.8 and 4.9.  $\square$

Finally, Hayashi *et al.* [23] and Even-Zohar *et al.* [16] describe infinite families of planar closed curves with defect  $\Omega(n^{3/2})$ ; see also [8, Section 2.2]. The following corollary is now immediate.

**Corollary 4.11.** Reducing any  $n$ -vertex planar graph to a single vertex requires  $\Omega(n^{3/2})$  planar electrical transformations in the worst case.

## 5 Open Problems

Our results suggest several open problems. Perhaps the most compelling, and the primary motivation for our work, is to find either a subquadratic upper bound or a quadratic lower bound on the number of (unrestricted) electrical transformations required to reduce any planar graph without terminals to a single vertex. Like Gitler [19], Feo and Provan [18], and Archdeacon *et al.* [3], we conjecture that  $O(n^{3/2})$  facial electrical transformations suffice. More ambitiously, we conjecture that any 2-terminal plane graph can be reduced to a single edge using  $O(n^{3/2})$  facial electrical transformations and terminal-leaf contractions, as mentioned in Section 3.3. However, proving these conjectures appears to be challenging.

Finally, none of our lower bound techniques imply anything about non-planar electrical transformations or about electrical reduction of non-planar graphs. Indeed, the only lower bound known in the most general setting, for any family of electrically reducible graphs, is the trivial  $\Omega(n)$ . It seems unlikely that planar graphs can be reduced more quickly by using non-planar electrical transformations, but we can't prove anything. Any non-trivial lower bound for this problem would be interesting.

## References

- [1] Virgil W. Adkisson. Cyclicly connected continuous curves whose complementary domain boundaries are homeomorphic, preserving branch points. *C. R. Séances Soc. Sci. Lett. Varsovie III* 23:164–193, 1930.
- [2] Francesca Aicardi. Tree-like curves. *Singularities and Bifurcations*, 1–31, 1994. Advances in Soviet Mathematics 21, Amer. Math. Soc.
- [3] Dan Archdeacon, Charles J. Colbourn, Isidoro Gitler, and J. Scott Provan. Four-terminal reducibility and projective-planar wye-delta-wye-reducible graphs. *J. Graph Theory* 33(2):83–93, 2000.
- [4] Vladimir I. Arnold. Plane curves, their invariants, perestroikas and classifications. *Singularities and Bifurcations*, 33–91, 1994. Adv. Soviet Math. 21, Amer. Math. Soc.
- [5] Vladimir I. Arnold. *Topological Invariants of Plane Curves and Caustics*. University Lecture Series 5. Amer. Math. Soc., 1994.
- [6] Jaizhen Cai. Counting embeddings of planar graphs using DFS trees. *SIAM J. Discrete Math.* 6(3):335–352, 1993.
- [7] Hsien-Chih Chang and Jeff Erickson. Electrical reduction, homotopy moves, and defect. Preprint, October 2015. arXiv:1510.00571.
- [8] Hsien-Chih Chang and Jeff Erickson. Untangling planar curves. *Proc. 32nd Int. Symp. Comput. Geom.*, 29:1–29:15, 2016. Leibniz International Proceedings in Informatics 51. (<http://drops.dagstuhl.de/opus/volltexte/2016/5921>).
- [9] Hsien-Chih Chang and Jeff Erickson. Unwinding annular curves and electrically reducing planar networks. Accepted to Computational Geometry: Young Researchers Forum, Proc. 33rd Int. Symp. Comput. Geom., 2017.
- [10] Hsien-Chih Chang, Jeff Erickson, David Letscher, Arnaud de Mesmay, Saul Schleimer, Eric Sedgwick, Dylan Thurston, and Stephan Tillmann. Tightening curves on surfaces via local moves. Submitted, 2017.
- [11] Yves Colin de Verdière, Isidoro Gitler, and Dirk Vertigan. Réseaux électriques planaires II. *Comment. Math. Helvetici* 71:144–167, 1996.
- [12] Lino Demasi and Bojan Mohar. Four terminal planar Delta-Wye reducibility via rooted  $K_{2,4}$  minors. *Proc. 26th Ann. ACM-SIAM Symp. Discrete Algorithms*, 1728–1742, 2015.
- [13] Giuseppe Di Battista and Roberto Tamassia. Incremental planarity testing. *Proc. 30th Ann. IEEE Symp. Foundations Comput. Sci.*, 436–441, 1989.
- [14] Giuseppe Di Battista and Roberto Tamassia. On-line planarity testing. *SIAM J. Comput.* 25(5):956–997, 1996.
- [15] G. V. Epifanov. Reduction of a plane graph to an edge by a star-triangle transformation. *Dokl. Akad. Nauk SSSR* 166:19–22, 1966. In Russian. English translation in *Soviet Math. Dokl.* 7:13–17, 1966.
- [16] Chaim Even-Zohar, Joel Hass, Nati Linial, and Tahl Nowik. Invariants of random knots and links. *Discrete & Computational Geometry* 56(2):274–314, 2016. arXiv:1411.3308.

- 1 [17] Thomas A. Feo. *I. A Lagrangian Relaxation Method for Testing The Infeasibility of Certain VLSI Routing*  
2 *Problems. II. Efficient Reduction of Planar Networks For Solving Certain Combinatorial Problems.*  
3 Ph.D. thesis, Univ. California Berkeley, 1985. (<http://search.proquest.com/docview/303364161>).
- 4 [18] Thomas A. Feo and J. Scott Provan. Delta-wye transformations and the efficient reduction of  
5 two-terminal planar graphs. *Oper. Res.* 41(3):572–582, 1993.
- 6 [19] Isidoro Gitler. *Delta-wye-delta Transformations: Algorithms and Applications.* Ph.D. thesis, Depart-  
7 ment of Combinatorics and Optimization, University of Waterloo, 1991.
- 8 [20] Isidoro Gitler and Feliú Sagols. On terminal delta-wye reducibility of planar graphs. *Networks*  
9 57(2):174–186, 2011.
- 10 [21] Maurits de Graaf and Alexander Schrijver. Making curves minimally crossing by Reidemeister  
11 moves. *J. Comb. Theory Ser. B* 70(1):134–156, 1997.
- 12 [22] Joel Hass and Peter Scott. Intersections of curves on surfaces. *Israel J. Math.* 51:90–120, 1985.
- 13 [23] Chuichiro Hayashi, Miwa Hayashi, Minori Sawada, and Sayaka Yamada. Minimal unknot-  
14 ting sequences of Reidemeister moves containing unmatched RII moves. *J. Knot Theory Ramif.*  
15 21(10):1250099 (13 pages), 2012. arXiv:1011.3963.
- 16 [24] Heinz Hopf. Über die Drehung der Tangenten und Sehnen ebener Kurven. *Compositio Math.*  
17 2:50–62, 1935.
- 18 [25] Arthur Edwin Kennelly. Equivalence of triangles and three-pointed stars in conducting networks.  
19 *Electrical World and Engineer* 34(12):413–414, 1899.
- 20 [26] Saunders Mac Lane. A structural characterization of planar combinatorial graphs. *Duke Math. J.*  
21 3(3):460–472, 1937.
- 22 [27] Steven D. Noble and Dominic J. A. Welsh. Knot graphs. *J. Graph Theory* 34(1):100–111, 2000.
- 23 [28] Michael Polyak. Invariants of curves and fronts via Gauss diagrams. *Topology* 37(5):989–1009,  
24 1998.
- 25 [29] Matthias F. M. Stallmann. Using PQ-trees for planar embedding problems. Tech. Rep. NCSU-CSC  
26 TR-85-24, Dept. Comput. Sci., NC State Univ., December 1985. ([https://people.engr.ncsu.edu/mfms/Publications/1985-TR\\_NCSU\\_CSC-PQ\\_Trees.pdf](https://people.engr.ncsu.edu/mfms/Publications/1985-TR_NCSU_CSC-PQ_Trees.pdf)).
- 27 [30] Matthias F. M. Stallmann. On counting planar embeddings. *Discrete Math.* 122:385–392, 1993.
- 28 [31] Ernst Steinitz. Polyeder und Raumeinteilungen. *Enzyklopädie der mathematischen Wissenschaften*  
29 *mit Einschluss ihrer Anwendungen* III.AB(12):1–139, 1916.
- 30 [32] Ernst Steinitz and Hans Rademacher. *Vorlesungen über die Theorie der Polyeder: unter Einschluß*  
31 *der Elemente der Topologie.* Grundlehren der mathematischen Wissenschaften 41. Springer-Verlag,  
32 1934. Reprinted 1976.
- 33 [33] Klaus Truemper. On the delta-wye reduction for planar graphs. *J. Graph Theory* 13(2):141–148,  
34 1989.
- 35 [34] Klaus Truemper. *Matroid Decomposition.* Academic Press, 1992.
- 36

- 1 [35] Donald Wagner. Delta-wye reduction of almost-planar graphs. *Discrete Appl. Math.* 180:158–167,  
2 2015.
- 3 [36] Hassler Whitney. Congruent graphs and the connectivity of graphs. *Amer. J. Math.* 54(1):150–168,  
4 1932.